

## Article

# Effect of Remelting Duration on Microstructure and Properties of SiC<sub>p</sub>/Al Composite Fabricated by Powder-Thixoforming for Electronic Packaging

Siyu Cai, Tijun Chen \* and Xuezheng Zhang

State Key Laboratory of Advanced Processing and Recycling of Nonferrous Metals, Lanzhou University of Technology, Lanzhou 730050, China; 13919466136@163.com (S.C.); zhangxz1991@163.com (X.Z.)

\* Correspondence: chentj@lut.cn; Tel.: +86-931-2976-573; Fax: +86-931-2976-578

Academic Editor: Hugo F. Lopez

Received: 30 August 2016; Accepted: 2 December 2016; Published: 8 December 2016

**Abstract:** In this work, a novel processing method called powder thixoforming was proposed to prepare composites reinforced with 50 vol % of SiC particles (SiC<sub>p</sub>) that were used for electronic packaging in order to investigate the effects of remelting duration on its microstructure and properties. Optical Microscope (OM), Scanning Electron Microscope (SEM), X-ray Diffraction (XRD) and Transmission Electron Microscope (TEM) methods were applied for the material characterization and the corresponding physical and mechanical properties were examined in detail. The obtained results indicate that the remelting duration exerted a large effect on the microstructure as well as the SiC<sub>p</sub>/Al interfacial reaction. The density and hardness of the composite continuously increased with increasing remelting duration. The thermal conductivity (TC) and bending strength (BS) first increased during the initial 90 min and then decreased. The remelting duration exerted a limited influence on the coefficient of thermal expansion (CTE). The optimal TC, BS, and hardness of these composites were up to 135.79 W/(m·K), 348.53 MPa, and 105.23 HV, respectively, and the CTE was less than 6.5 ppm/K after the composites were remelted at 600 °C for 90 min. The properties of the composites could thus be controlled to conform to the application requirements for electronic packaging materials.

**Keywords:** particle-reinforced composites; powder thixoforming; microstructure; thermo-physical properties; mechanical properties

## 1. Introduction

Composites of Al and a high volume fraction of SiC particles are expected to develop into one of the most widely used electronic packaging or thermal management materials because of their excellent thermal and mechanical properties, such as low coefficient of thermal expansion, high thermal conductivity, high modulus, and low density [1–6]. So far, several methods have been developed to fabricate this kind of composites, for instance, squeeze casting, powder metallurgy (PM), and vacuum/pressure infiltration. However, all of these methods have obvious shortcomings. As the main method used to fabricate high-volume-fraction-SiC<sub>p</sub>/Al composites (SiC<sub>p</sub> is short for SiC particles), vacuum/pressure infiltration can produce SiC<sub>p</sub>/Al composites with high performance and low porosity, but the cost of equipment and molds is quite high. Besides, the technical procedure is long, and the process implementation is relatively complex [7–9]. Nevertheless, as a novel technology for preparing particle-reinforced metal composites that combines the merits of powder metallurgy and thixoforming, powder thixoforming (PTF) has many advantages such as uniform particle distribution, compact microstructure, and near-net-shape components with complex geometries [10,11]. The blending and pressing steps of PM are utilized to prepare ingots with

high volume fraction and uniform distribution of reinforcing particles in the matrix; the ingots are then partially remelted and thixoformed. This technology can be expected to produce composite components with uniform distribution of reinforcing particles as well as few or no voids. At the same time, the process is simple and thus the cost is comparatively lower than that of vacuum/pressure infiltration technology. Unfortunately, most published research on PTF focused mainly on the microstructural evolution during partial remelting [12] and mechanical properties of the resulting composites [13]. More recently, Li et al. [14] applied PTF to fabricate SiC<sub>p</sub>/2024 Al-based composites and investigated the effects of mold temperature on its microstructure and tensile properties. Moreover, Zhang et al. [15] utilized the same PTF method to produce SiC<sub>p</sub>/6061 Al composites and studied the effects of solution treatment on its tensile properties, and the corresponding strengthening mechanisms were also quantitatively discussed. However, most of the aforementioned researches were concerned about the composites with a low volume fraction of SiC particles. Only a few studies involved high-volume-fraction-SiC<sub>p</sub>/Al composites fabricated by PTF, but they concentrated on the effects of parameters, such as content of alloying elements, remelting temperature [16], and ratio of reinforcement particles with different sizes [17], on the microstructure and properties of the resulting composites. Relatively little attention has been paid to the remelting duration, which can be a very important factor in the interfacial reaction between the SiC particles and Al. The objective of this paper was to report the effect of remelting duration on the microstructures, thermal physical properties and mechanical properties of PTF SiC<sub>p</sub>/Al composites. The obtained results shed light on the optimal remelting duration under which the properties of the composites could thus be controlled to conform with the application requirements for electronic packaging materials.

## 2. Materials and Methods

### 2.1. Fabrication of SiC<sub>p</sub>/Al Composites

In this study, Al–13Si (wt %) alloy powder with a particle size of 20 µm (Changfeng factory, Lanzhou, China) and SiC particles with an average particle size of 100 µm (Changfeng factory, Lanzhou, China) were used as the matrix and reinforcements, respectively. To remove surface impurities from the SiC particles, they were washed with a solution of 10% hydrochloric acid (Kejia Chemical Company, Ningbo, China). The particles were then cleaned with distilled water 3–4 times and dried at 140 °C (the oxidization onset temperature of SiC was evidenced to be 800–850 °C [18]) for 12 h in order to fully eliminate the used water. The chemical compositions of the SiC particles and Al–Si alloy powder are given in Table 1.

**Table 1.** Chemical compositions of the used SiC<sub>p</sub> and Al alloy powders.

SiC <sub>p</sub>				Alloy Powders			
SiC	Fe	Si	O	Al	Fe	Si	Cu
97.2%	1.14%	0.98%	0.35%	86.82%	0.106%	13.06%	0.0006%

The aluminum–silicon alloy powder and SiC particles were mixed at a 50:50 volume ratio in an ND7-21 planetary ball-milling machine (Nanjing Laibu Technology Industry Co., Ltd., Nanjing, China) at a rotation speed of 120 rad/min for 40 min. Specimens with dimensions of Φ45 mm × 30 mm were used as the starting ingots of thixoforming; they were obtained by cold pressing the mixed powder under an optimized pressure of 140 MPa on a hydraulic machine. The ingots were heated in a vacuum resistance furnace for different durations ranging from 45 to 120 min at 600 °C. The heated ingots were then quickly transferred to a forging mold (Changfeng factory, Lanzhou, China) with a cavity of Φ45 mm × 70 mm and forged under a pressure of 120 MPa. Thixoformed products prepared with different remelting durations were obtained.

## 2.2. Material Characterization

Subsequently, all kinds of specimens used in this work were machined from the central region of these thixoformed products. Specimens with dimensions of  $\Phi 12.5 \text{ mm} \times 2.5 \text{ mm}$  were used for thermal conductivity (TC) measurements with a laser flash thermal analyzer (LFA 457, NETZSCH, Bavaria, Germany); Specimens with dimensions of  $3 \text{ mm} \times 4 \text{ mm} \times 25 \text{ mm}$  were used for measurements of the coefficient of thermal expansion (CTE) with a thermal dilatometer (DIL 402EP, NETZSCH, Bavaria, Germany); Both of three tests were averaged for TC and CTE in this work. Specimens with dimensions of  $4 \text{ mm} \times 5 \text{ mm} \times 35 \text{ mm}$  were used to examine variations in their bending strength (BS) with a universal material testing machine (AG-10TA, Shimadzu, Kyoto, Japan) by using a three-point bending test, and five values were averaged for each composite.

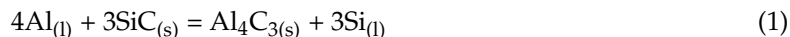
The microstructure and fractography of the specimens were observed on a MeF3 optical microscope (OM; Nikon Instruments, Shanghai, China), a QUANTA FEG 450 scanning electron microscope (SEM; FEI, Hillsboro, OR, USA), and a high-resolution transmission electron microscope (TEM; JEM-2010, JEOL, Akishima, Japan). TEM foils were prepared by standard mechanical and ion-beam thinning techniques using a Gatan-691 precision ion polishing system with liquid-nitrogen cooling. The hardness were examined using an optical Brinell–Rockwell–Vickers hardness tester (HBRVU-187.5, Shanghai, China). The obtained OM images were analyzed by Image-Pro Plus 6.0 software (Media Cybernetics Company, Silver Spring, MD, USA), and the ratio of the pore area to the entire area was defined as the pore content. The average of five hardness measurements at different locations of each specimen was used as the hardness of the thixoforged product. Some typical fracture surfaces and their side views were observed with the SEM. The Archimedes method was utilized to measure the density of the products and the measuring details can be found elsewhere [19].

## 3. Results and Discussion

### 3.1. Microstructure

Typical OM micrographs of the resulting  $\text{SiC}_p/\text{Al}$  composites are presented in Figure 1, demonstrating that the SiC particles were uniformly distributed in the Al matrix in all of the products. The pore content (marked by arrows) obviously decreased with increasing remelting duration. The quantitative examination results in Table 2 more clearly present this trend. In addition, the pores' size also decreased as remelting duration increased (Table 2). In other words, the compactness of the microstructure was improved by increasing the melting time, which can be evidenced by the relative density (Table 2).

It should be noted that prolonging the remelting duration could enhance the microstructure's compactness, but this could also promote an interfacial reaction between the Al melt and SiC particles as follows:



Owing to the interfacial reaction between Al melt and SiC, an increase in remelting duration was expected to enhance the fluidity of the Al melt and the wettability by SiC particles by decreasing the contact angle between SiC particles and the Al melt [20], since the increase in Si content resulting from the interfacial reaction tend to degrade the viscosity of the liquid and the transformation of the interface between SiC particles and Al melt was also caused by the reaction, which would improve the infiltration of the melt into the pores between the SiC particles during the remelting stage and the subsequent thixoforging stage, consequently reducing the amount of pores in the obtained composite.

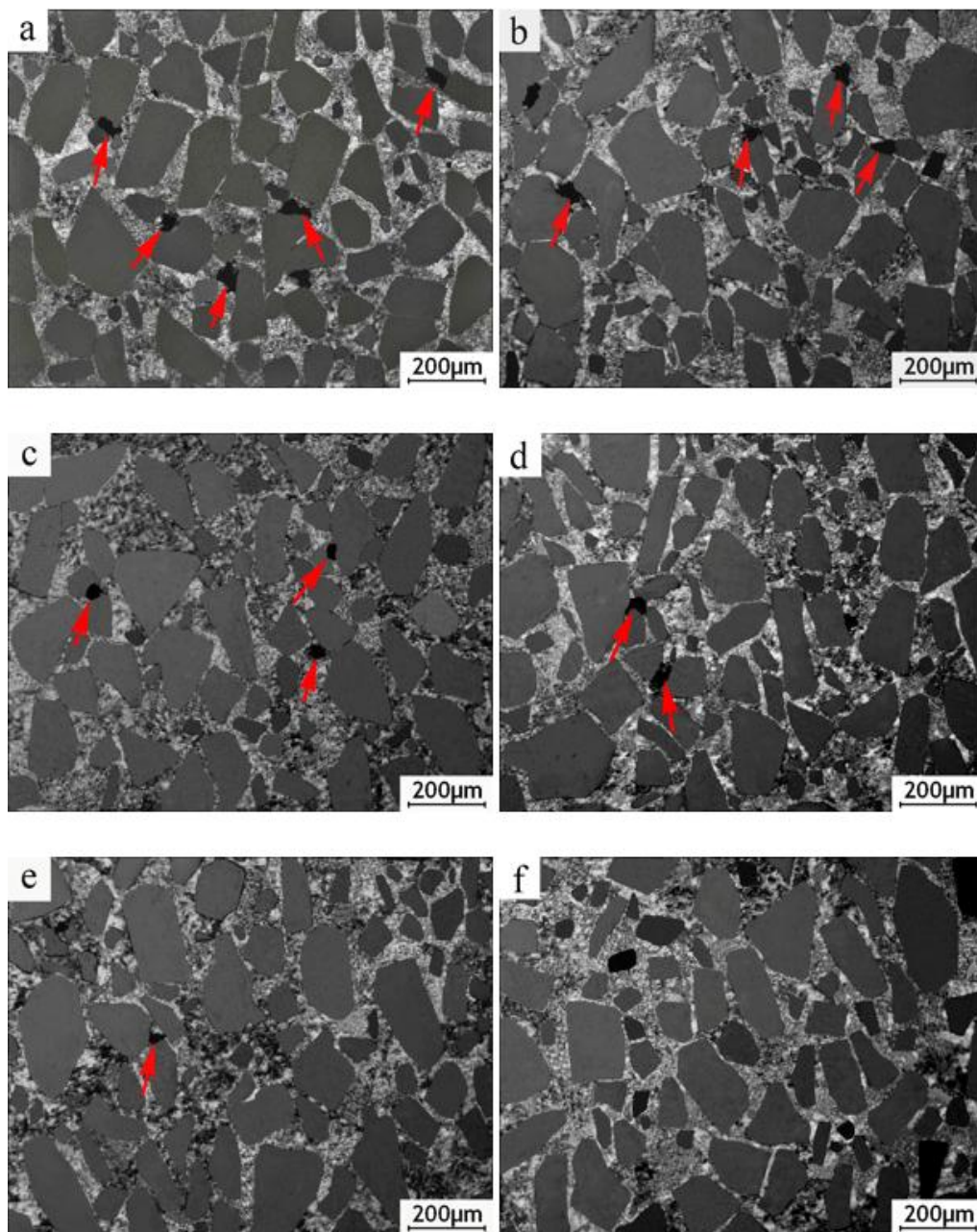


**Figure 1.** OM micrographs of the SiC<sub>p</sub>/Al composites thixoformed under remelting at 600 °C for (a) 45 min; (b) 60 min; (c) 75 min; (d) 90 min; (e) 105 min; and (f) 120 min (The red arrows indicate the pores in the microstructure of these composites).

**Table 2.** Density, pore size and pore volume fraction of SiC<sub>p</sub>/Al composites.

Remelting Duration (min)	Pore Size (μm)	Pore (%)	Density (%)
45	38.537	8.64	90.2
60	32.334	4.71	93.1
75	28.392	2.37	96.4
90	20.433	1.96	97.3
105	18.138	0.93	98.5
120	-	-	99.2



As seen in Figure 1, the morphology of the SiC particles changed from the original multi-angled shape to a spheroidal structure as the remelting duration increased. This indicates that the SiC particles were corroded by the Al melt and the interfacial reaction occurred in the composites during the remelting process, especially the one with a long remelting duration. Figure 2 depicts the XRD patterns of the composites corresponding to those in Figure 1. The peak of the  $\text{Al}_4\text{C}_3$  crystal appeared until the remelting duration was extended to 105 min, and it should be observed that such  $\text{Al}_4\text{C}_3$  peak of the composite remelted for 120 min is much higher than the one remelted for 105 min, indicating that the longer remelting duration led to the more serious reaction shown in Equation (1). The generated  $\text{Al}_4\text{C}_3$  could not only react with the atmospheric moisture to degrade the properties of the composites, but also offer interfacial thermal resistance to reduce the TC of the composites by 20%–30% depending on the extent of the reaction [21–23]. Moreover, Masayuki et al. [24] further indicated that a strong interface bonding resulted from the tendency for the  $\text{Al}_4\text{C}_3$  reaction layer to form a semi-coherent interface with the aluminum matrix, and it can be deduced that the semi-coherent interface should give rise to the increase of interfacial thermal resistance to reduce the TC of the composites. Therefore, the composite remelted at 90 min can be expected to exhibit the optimal TC value because few amount of pores and interfacial reaction products occurred in the composite remelted for 90 min.

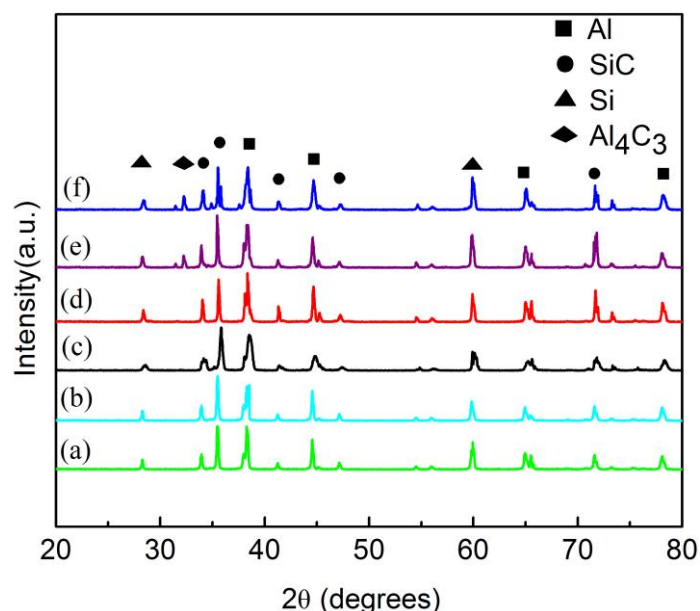


**Figure 2.** XRD patterns of the composites thixoformed under reheating for (a) 45; (b) 60; (c) 75; (d) 90; (e) 105; and (f) 120 min.

Figure 3 shows TEM micrographs and corresponding diffraction patterns of products generated at the interface after being remelted for 90 and 105 min. Figure 3a shows a clear and smooth  $\text{SiC}_p/\text{Al}$  interface, indicating that the interfacial reaction is not serious because the products of the interfacial reaction can not be clearly observed during the relatively shorter duration of 90 min. Moreover, when the remelting duration was further extended to 105 min, the edges of the SiC particles were severely eroded by the aluminum alloy, as shown in Figure 3b, and the  $\text{SiC}_p/\text{Al}$  interface was quite rough. Many needle-like  $\text{Al}_4\text{C}_3$  crystals (marked by arrows in Figure 3b) were attached parallel to the  $\text{SiC}_p/\text{Al}$  interface. The corresponding diffraction patterns shown in Figure 3b also confirm the existence of  $\text{Al}_4\text{C}_3$  in this composite after a remelting duration of 105 min. This is consistent with report by Shi et al. [25] that longer holding time led to larger reaction degree between  $\text{SiC}_p$  and Al. Results from earlier studies [26,27] disclosed that the formation mechanism of  $\text{Al}_4\text{C}_3$  crystals is based on such a concentration gradient that leads to possible further consumption of SiC and further growth of  $\text{Al}_4\text{C}_3$  crystals by migration of carbon atoms, which diffuse in the liquid phase.

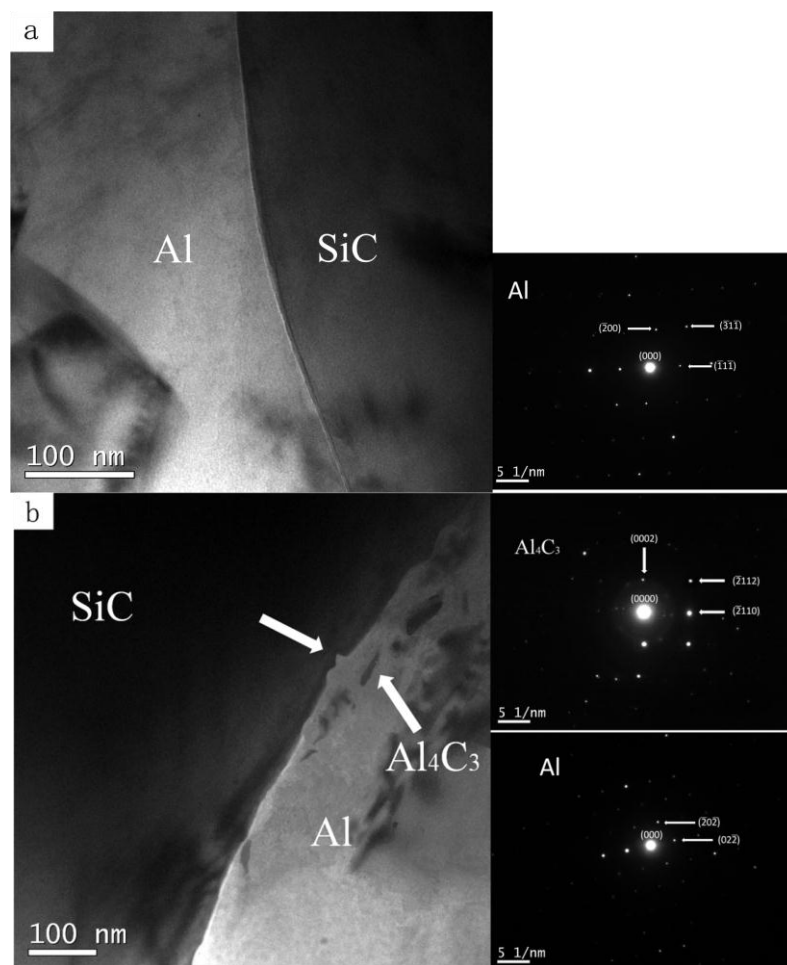


**Figure 3.** TEM micrographs and diffraction patterns of the SiC<sub>p</sub>/Al interface at the remelting duration of (a) 90 min; and (b) 105 min.

In summary, the extension of the remelting duration could decrease the amount of pores in the composite microstructure and thus enhance its density. The composite that remelted at 90 min can be expected to exhibit the optimal TC value because the low amount of pores existed in this composite and no excessive interfacial reaction occurred. However, further enhanced remelting after 90 min could promote the formation of harmful Al<sub>4</sub>C<sub>3</sub> near the SiC<sub>p</sub>/Al interface, which could decrease the TC.

### 3.2. Thermal Physical Properties

#### 3.2.1. Thermal Conductivity of SiC<sub>p</sub>/Al Composites

The experimental values of TC of the SiC<sub>p</sub>/Al composites are plotted in Figure 4. TC first increased during the period of 45 to 90 min, reached the maximum value of 135.79 W/(m·K) at 90 min, and decreased thereafter. As reported in a previous research, electronic packaging technology requires a minimum TC of 100 W/(m·K) [28]. Therefore, the obtained composite remelted for 90 min could fully meet this requirement.

In an attempt to gain a theoretical understanding of the effect of remelting duration on the TC of the SiC<sub>p</sub>/Al composites, a model proposed by Hasselman and Johnson (H-J model), which has been widely used for the TC prediction of particle-reinforced composite [29], was utilized to predict the

TC of the present composites. Hasselman and Johnson have shown that the TC of a composite with continuous matrix and dilute volume fraction of spherical reinforcements can be expressed as follows:

$$K_c = K_m^{\text{eff}} \frac{[2K_m^{\text{eff}} + K_r^{\text{eff}} + 2(K_r^{\text{eff}} - K_m^{\text{eff}}) \cdot V_r]}{2K_m^{\text{eff}} + K_r^{\text{eff}} - (K_r^{\text{eff}} - K_m^{\text{eff}}) \cdot V_r} \quad (2)$$

where  $K_r^{\text{eff}}$  is the efficient TC of the reinforcements, and it can be calculated with the following equation

$$K_r^{\text{eff}} = \frac{K_r a h_c}{a h_c + K_r} \quad (3)$$

where  $K$  represents the TC; the subscripts  $c$ ,  $m$ , and  $r$  refer to the composites, matrix (167 W/(m·K) [30]), and reinforcements (185 W/(m·K) [31]), respectively;  $V_r$  is the volume fraction of reinforcements ( $V_{\text{SiC}}$ );  $a$  is the radius of the spherical reinforcements (50  $\mu\text{m}$ ); and  $h_c$  is the thermal boundary conductance.

In order to measure the true volume fraction of SiC particles in each thixoformed composite, cubic specimens with dimensions of 1 cm  $\times$  1 cm  $\times$  1 cm were cut from the central parts of each composite reheated for 45–120 min. The geometric dimension of these obtained samples ( $V_c$ ) were measured again by utilizing the vernier caliper to obtain the accurate values of each composites' volume. These samples were then placed into the industrial 40% HF solution (considering that only the HF solution can dissolve Si phase among all the acid solutions) to fully dissolve all the phases consist in the composites except the SiC. Subsequently, the SiC particles were filtrated from the acid solution with the filter paper which was measured to obtain the mass of each paper ( $M_f$ ). The mixture of filter paper and SiC particles were dried and their mass ( $M_m$ ) can thus be obtained. In this way, the mass of SiC particles ( $M_{\text{SiC}}$ ) in the different samples can be measured by:  $M_{\text{SiC}} = M_m - M_f$ . Three specimens were averaged for each sample. The volume of SiC ( $V_{\text{SiC}}$ ) can be obtained by:  $V_{\text{SiC}} = M_{\text{SiC}} / \rho_{\text{SiC}}$  ( $\rho_{\text{SiC}} = 3.23 \text{ g/cm}^3$  [31]). According to the volume of SiC particles and each sample, the volume fraction of SiC particles in the resultant composites can be calculated. The experimental values of the  $M_{\text{SiC}}$ ,  $V_{\text{SiC}}$  and volume fraction of SiC in each composites remelted for 45–120 min are depicted in Table 3. The data listed in Table 3 suggested a decrease in the volume fraction of SiC particles when prolonging the remelting duration, due mainly to the gradually enhanced interfacial reactions which could consume certain amounts of SiC particles as a function of remelting duration.

**Table 3.** The experimental  $M_{\text{SiC}}$ , calculated  $V_{\text{SiC}}$ ,  $V_c$  and the volume fraction of SiC.

Remelting Duration (min)	$M_{\text{SiC}}$ (g)	$V_{\text{SiC}}$ (cm <sup>3</sup> )	$V_c$ (cm <sup>3</sup> )	SiC Vol %
45	1.7283 $\pm$ 0.0087	0.535	1.078	49.63
60	1.5782 $\pm$ 0.0031	0.489	0.987	49.54
75	1.7606 $\pm$ 0.0105	0.545	1.104	49.37
90	1.6121 $\pm$ 0.0048	0.499	1.016	49.11
105	1.6156 $\pm$ 0.0056	0.500	1.025	48.78
120	1.5584 $\pm$ 0.0043	0.483	0.998	48.40

More recently, Molina et al. [32] modified the H–J model into a two-step H–J model, and Chu et al. [33] proposed a method called multiple effective media approximation (MEMA) to more precisely calculate TC. They treated the pores as a non-thermally conducting inclusion in the metal matrix, and accordingly, the composites were composed of reinforcements and a pore-containing matrix. Hence,  $K_m^{\text{eff}}$  in Equation (2) can be calculated from

$$K_m^{\text{eff}} = \frac{K_m (2 - 2 \cdot V_p)}{2 + V_p} \quad (4)$$

where  $V_p$  is the volume fraction of pores.

The value of  $h_c$  of the SiC<sub>p</sub>/Al composites was about  $7.10 \times 10^7$  W/(m<sup>2</sup>·K) [26–28]. Figure 4 shows the theoretically calculated data along with the experimental values of TC at different remelting durations. The calculated values of TC increase first with prolonging the remelting duration and then decrease after 90 min, and are found to have the same variation tendency with the experimental values.

The above theoretical calculation implied that the TC was considerably affected by the pores in the composites because the TC of pores was very low [20,34]. A quantitative examination showed that the pore content continuously decreased when the remelting duration increased from 45 to 90 min (Table 2), accounting for the slight TC increase as the remelting duration was prolonged from 45 to 90 min. Further extension of the remelting duration degraded the TC owing to the enhanced effect of serious interfacial scattering counteract the beneficial effect of decreasing pore content on TC, which was closely related to the larger amount of generated Al<sub>4</sub>C<sub>3</sub> near the SiC<sub>p</sub>/Al interface and resulted in an increase in interfacial thermal resistance.

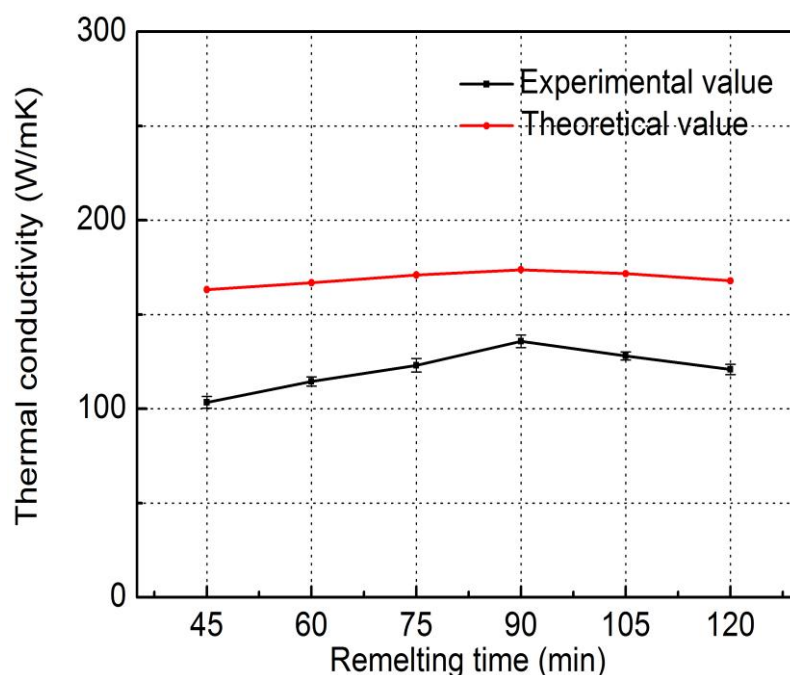


**Figure 4.** Theoretical and experimental TC of the SiC<sub>p</sub>/Al composites thixoformed under different remelting durations.

It must be noted that the experimental TC values are somewhat lower than the calculated data. There are several possible reasons for this discrepancy. First, the modified H–J model was derived from the H–J model (Equation (2)), however, the microstructure of the present composites was inconsistent with the assumed microstructure in the H–J model. The shape of the SiC particles used in the experiments was not spherical and their volume fraction was quite high. Second, in the modified H–J model, it is presumed that pores exist merely in the matrix and the TC of pores is zero. In this work, however, most of pores existed in the vicinity of SiC particles, as shown in Figure 1, indicating that the SiC<sub>p</sub>/Al interface was separated by the pores. It is believed that the thermal scattering by the separated interface was considerable compared to that of pores in the matrix [28,34]. Moreover, the generated Al<sub>4</sub>C<sub>3</sub> was detrimental to TC since it can react with the atmospheric moisture and offer interfacial thermal resistance to reduce the TC of these composites. The aforementioned reasons could account for the lower experimental values as compared to the calculated theoretical data.

In brief, the experimental TC first increased during the period of 45–90 min owing to the decrease in the amount of pores and reached the maximum value of 135.79 W/(m·K) at 90 min. It then degraded because of the decrease in SiC volume fraction and the promoted formation of Al<sub>4</sub>C<sub>3</sub> resulted



from the further enhanced interfacial reaction. The calculated TC data from the modified H–J model were always higher than the experimental values regardless of the remelting duration.

### 3.2.2. Coefficient of Thermal Expansion of SiC<sub>p</sub>/Al Composites

Figure 5 depicts the experimental values of CTE for composites prepared with different remelting durations. These values were in the range of 6–9 ppm/K, which demonstrated that the CTE values were actually unrelated to the remelting duration. In other words, the CTE values were irrelevant to the volume of pores and the interfacial reaction. The findings of a previous study, which suggested that the CTE of a composite is relatively insensitive to the pores in the microstructure with a continuous metallic phase [35], are consistent with the results of the present work.

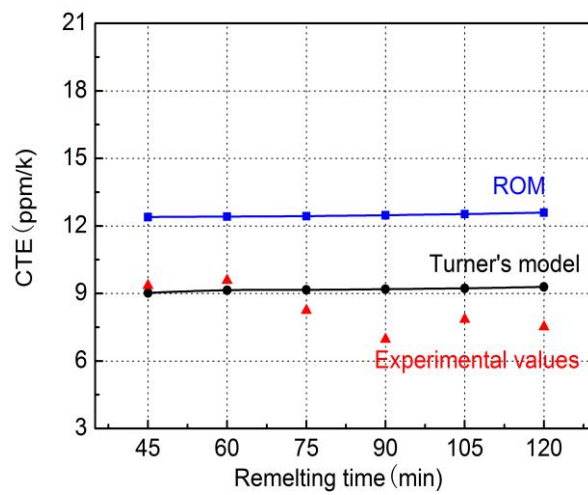


**Figure 5.** Variations of the CTE of the composites obtained from ROM, Turner's model and experimental results as a function of remelting duration.

Several models can be used to theoretically predict the CTE of the SiC<sub>p</sub>/Al composites. The most commonly used models include one based on the rule of mixture (ROM) and Turner's model [36]. According to the ROM, the CTE can be expressed as

$$\alpha_c = \alpha_m V_m + \alpha_r V_r \quad (5)$$

while according to Turner's model, it can be expressed as

$$\alpha_c = \frac{\alpha_m V_m k_m / \rho_m + \alpha_r V_r k_r / \rho_r}{V_m k_m / \rho_m + V_r k_r / \rho_r} \quad (6)$$

where  $\alpha$  is the CTE;  $V$  is the volume fraction;  $K$  is the modulus;  $\rho$  is the density; and subscripts c, m, and r refer to the composite, matrix, and reinforcements (SiC<sub>p</sub>), respectively. The value of  $\alpha$  of the SiC particles was 4.7 ppm/K [37] and that of the AlSi13 alloy was 19.975 ppm/K [30]. The values of  $K$  of SiC particles and the AlSi13 alloy were 227 and 76.21 GPa, respectively [30,37]. Substituting  $\rho$  of 3.2 and 2.674 g/cm<sup>3</sup> for SiC and AlSi13 into these two equations, the calculated CTE by ROM and Turner's model are 12.39–12.59 ppm/K and 9.12–9.29 ppm/K respectively, regarding the true volume fraction of each phase related to different remelting duration.

Figure 5 also depicts the calculated data obtained from ROM and Turner's model along with the experimental values of CTE of composites prepared with different remelting durations. It is evident that the calculated data from Turner's model are much more consistent with the experimental values than those from the ROM. This can be attributed to the simple and rigid combination of the CTE values of the matrix and reinforcements in the ROM [38,39], and the disregard for the modulus

difference between the matrix and reinforcements in the ROM. Therefore, in view of the present results, Turner's model should be applied to better predict the CTE of high-volume-fraction particle-reinforced composites. It was reported in a previous study that Turner's model is appropriate for predicting the CTE of low-volume-fraction particle-reinforced Al–Si matrix composites [40]. The present work also confirms that Turner's model can be utilized to predict the CTE of high-volume-fraction composites.

In short, the CTE values of  $\text{SiC}_p/\text{Al}$  composites were actually unrelated to the remelting duration and varied in the range of 6–9 ppm/K. The data calculated from Turner's model are much more consistent with the experimental values than those from the ROM in the present work.

### 3.3. Mechanical Properties of $\text{SiC}_p/\text{Al}$ Composites

High mechanical properties are also required for the use of  $\text{SiC}_p/\text{Al}$  composites as electronic packaging material to avoid damage from the pressing, shaking, and impact during the process of assembly and carriage. Figure 6 shows the variations in BS and hardness of the composite with remelting duration. The BS value of the thixoformed composite exhibited an increase from 299.83 to 348.53 MPa as the remelting duration was extended from 45 to 90 min. Further extending the remelting duration decreased the BS from 348.53 to 335.91 MPa. In general, the macro-mechanical properties of composites are closely related to the mechanical properties of each constituent and the matrix–reinforcement interfacial bonding. The high-volume-fraction  $\text{SiC}_p/\text{Al}$  composites with brittle SiC particles and a plastic Al matrix were beneficial to the release of stress concentration at the  $\text{SiC}_p/\text{Al}$  interface by plastic deformation of the Al matrix and to coordination of the deformation of the composites. The pores that existed in the composites were detrimental to their mechanical properties. As mentioned in Section 3.1, the pore content decreased and the microstructure compactness was improved as the remelting duration increased to 90 min. The values of BS and hardness also continuously increased. However, when the remelting duration exceeded 90 min, the BS value decreased as a result of the effects of the further formation of brittle  $\text{Al}_4\text{C}_3$ , which was detrimental to BS. However, since the brittle  $\text{Al}_4\text{C}_3$  was beneficial to hardness, the hardness continued to increase after 90 min. Furthermore, in comparison with the lowest BS of the composites remelted for 45 min and the highest one for 90 min, it should be noted that a decrease of 6.7% in porosity (8.64% to 1.96%) induced an enhancement in BS lower than 15% (299.83 to 348.53 MPa). The reason was that the decrease of pores resulted in the augment of BS while the formation of  $\text{Al}_4\text{C}_3$  was detrimental to the BS. Therefore, it is just due to the counteraction and the combined effects of aforementioned two factors that the difference of BS between the composites remelted for 45 and 90 min was rather limited.

Figure 7 shows the fracture surfaces of the composites thixoformed after different remelting durations. Numerous pores existed in the vicinity of the SiC particles (marked by arrows in Figure 7a) when the remelting duration was 45 min. In contrast, the SiC particles were surrounded by the ductile matrix of the composite thixoformed after a remelting duration of 90 min and only a few pores were found at the SiC/matrix interface (Figure 7b). As the remelting duration increased to 120 min, no pores were found (Figure 7c), demonstrating that the microstructure compactness was gradually improved with increasing the remelting duration. In addition, the SiC particles exhibited two-way behavior, fracture and debonding of the  $\text{SiC}_p/\text{Al}$  interface, regardless of the remelting duration. These two types of behavior contributed to the concentration of stress generated during bending tests at the  $\text{SiC}_p/\text{Al}$  interface [41].

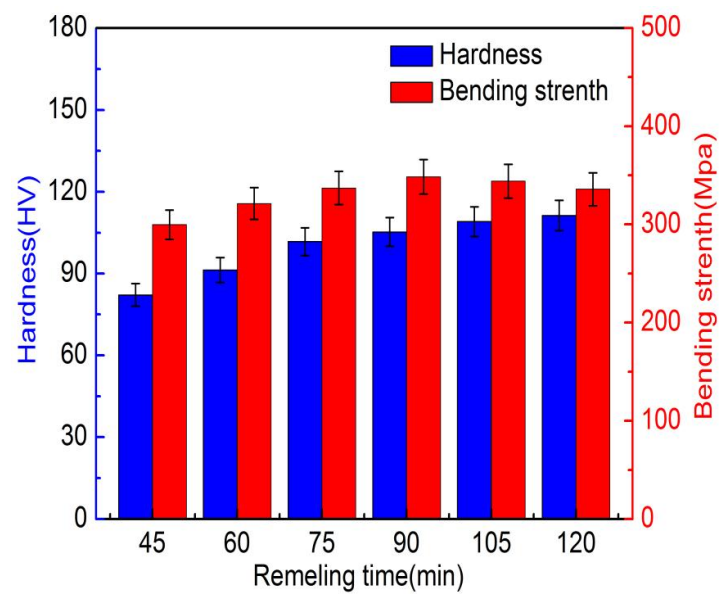


**Figure 6.** Bending strength and hardness of the composite thixoformed at different remelting durations.

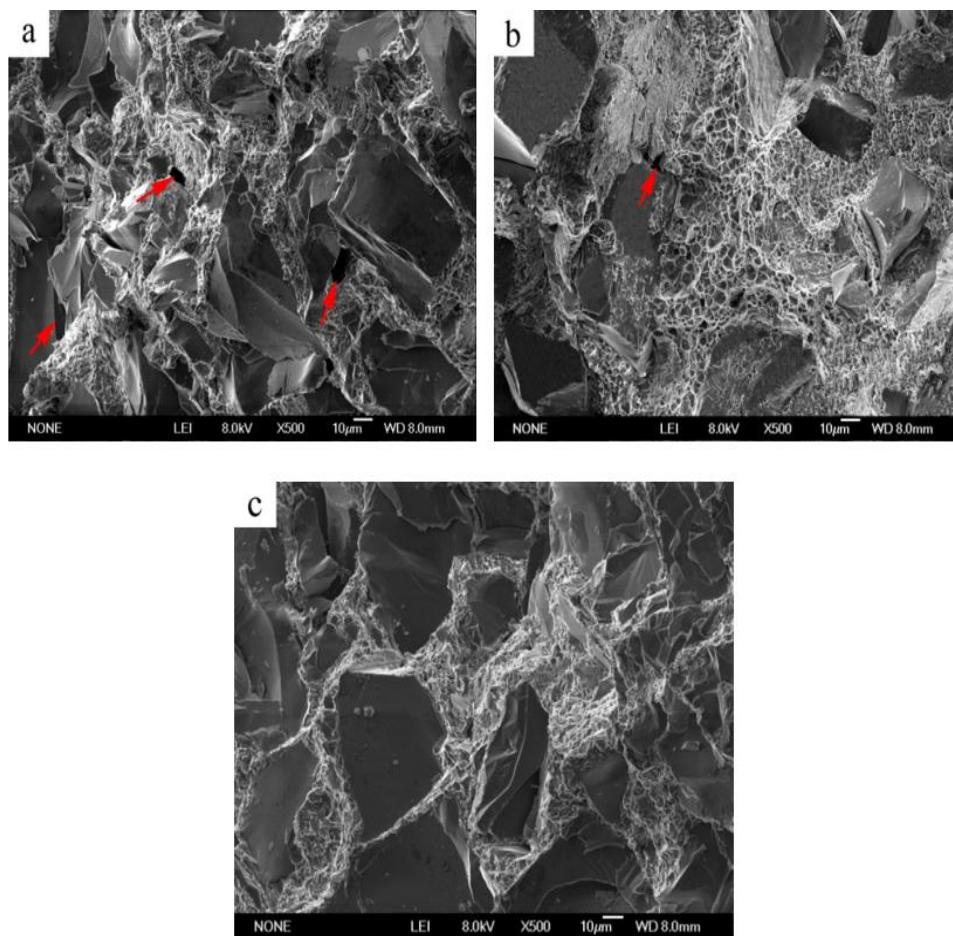


**Figure 7.** Fracture surfaces of the SiC<sub>p</sub>/Al composite thixoformed at the remelting durations of (a) 45 min, (b) 90 min; and (c) 120 min (The red arrows indicate the pores on the fracture surfaces of these composites).

Overall, the BS and hardness continuously increased from 45 to 90 min because of the gradually reduced pore content. Further extension of the remelting duration beyond 90 min decreased the BS yet enhanced the hardness because of the formation of brittle  $\text{Al}_4\text{C}_3$ . The corresponding fracture surfaces of the composites with different remelting durations confirm the variations in pores, as discussed earlier.

#### 4. Conclusions

The main results of this work are summarized as follows:

- (1) The extension of the remelting duration could decrease the number of pores in the composite microstructure and enhance its density. The composites remelted at 90 min exhibited the optimal TC value because no excessive interfacial reaction occurred. However, further increased remelting duration could promote the formation of harmful  $\text{Al}_4\text{C}_3$  near the  $\text{SiC}_p/\text{Al}$  interface, which could decrease the TC.
- (2) The experimental TC first increased during the period from 45 to 90 min owing to the reduced pore content and reached the maximum value of 135.79 W/(m·K) at 90 min. It then decreased because of the interfacial reaction. The calculated TC data from the modified H–J models are always higher than the experimental values regardless of the remelting duration.
- (3) The CTE values of  $\text{SiC}_p/\text{Al}$  composites were actually unrelated to the remelting duration and varied in the range of 6–9 ppm/K. The calculated data from Turner’s model are much more consistent with the experimental values than those from the ROM in the present work.
- (4) The BS and hardness continuously increased from 45 to 90 min owing to the gradually reduced pore content. Further extension of the remelting duration beyond 90 min decreased the BS and enhanced the hardness because of the formation of brittle  $\text{Al}_4\text{C}_3$ .

**Acknowledgments:** The authors wish to express thanks for financial support from the Basic Scientific Fund of Gansu Universities (Grant No. G2014-07), the Program for New Century Excellent Talents in University of China (Grant No. NCET-10-0023) and the Program for Hongliu Outstanding Talents of Lanzhou University of Technology (Grant No. 2012-03).

**Author Contributions:** Siyu Cai did the experiments and data analysis and wrote the paper. Tijun Chen reviewed and revised the manuscript of this paper. Xuezheng Zhang contributed to the data analysis.

**Conflicts of Interest:** The authors declare no conflict of interest.

#### References

1. Mohn, W.R.; Vukobratovich, D. Recent applications of metal matrix composites in precision instruments and optical systems. *J. Mater. Eng.* **1988**, *10*, 225–235. [[CrossRef](#)]
2. Jin, S. Advances in thermal management materials for electronic applications. *JOM* **1998**, *50*, 46. [[CrossRef](#)]
3. Rawal, S.P. Metal-matrix composites for space applications. *JOM* **2001**, *53*, 14–17. [[CrossRef](#)]
4. Miracle, D.B. Metal matrix composites—From science to technological significance. *Compos. Sci. Technol.* **2005**, *65*, 2526–2540. [[CrossRef](#)]
5. Cui, Y.; Wang, L.; Ren, J. Multi-functional  $\text{SiC}/\text{Al}$  composites for aerospace applications. *Chin. J. Aeronaut.* **2008**, *21*, 578–584.
6. Beelen-Hendrikx, C.; Verguld, M. Trends in electronic packaging and assembly for portable consumer products. In Proceedings of the 3rd Electronics Packaging Technology Conference, Sheraton Towers, Singapore, 5–7 December 2000; pp. 24–32.
7. Prabu, S.B. Effect of the squeeze pressure on the mechanical properties of the squeeze cast  $\text{Al}/\text{SiC}_p$  metal matrix composite. *Int. J. Met.* **2013**, *8*, 299–312.
8. Bishop, D.P.; Caley, W.F.; Kipouros, G.J.; Hexemer, R.L.; Donaldson, I.W. Powder metallurgy processing of 2xxx and 7xxx series aluminium alloys. *Can. Metall. Q.* **2011**, *50*, 246–252. [[CrossRef](#)]
9. Liu, M.T.; Cai, X.S.; Li, G.Q. Microstructure and thermal properties of high-performance  $\text{SiC}$  reinforced  $\text{Al}$  matrix composite. *Trans. Nonferr. Met. Soc. China* **2013**, *23*, 1040–1046.
10. Jung, H.K.; Kang, C.G. A study on a thixoforming process using the thixotropic behavior of an aluminum alloy with an equiaxed microstructure. *J. Mater. Eng. Perform.* **2000**, *9*, 530–535.

11. Li, Y.; Liu, X.; Zhang, X.; Zhou, H. A review of semi-solid near-net forming in wrought aluminum alloy. *Spec. Cast. Nonferr. Alloy.* **2014**, *34*, A28. (In Chinese)
12. Li, P.B.; Chen, T.J.; Zhang, S.Q.; Wang, Y.J. Effects of partial remelting on the microstructure evolution of SiC<sub>p</sub>/2024 aluminum composites prepared by alloy powder cold pressing. *Spec. Cast. Nonferr. Alloy.* **2015**, *35*, 260–263.
13. Ferreira, L.M.P.; Robert, M.H.; Bayraktar, E.; Zaimova, D. New design of aluminium based composites through combined method of powder metallurgy and thixoforming. *Adv. Mater. Res.* **2014**, *939*, 68–75. [[CrossRef](#)]
14. Li, P.B.; Chen, T.J.; Qin, H. Effects of mold temperature on the microstructure and tensile properties of SiC<sub>p</sub>/2024 Al-based composites fabricated via powder thixoforming. *Mater. Des.* **2016**, *112*, 34–45. [[CrossRef](#)]
15. Zhang, X.Z.; Chen, T.J.; Qin, Y.H. Effects of solution treatment on tensile properties and strengthening mechanisms of SiC<sub>p</sub>/6061Al composites fabricated by powder thixoforming. *Mater. Des.* **2016**, *99*, 182–192. [[CrossRef](#)]
16. Guo, M.H.; Liu, J.Y.; Jia, C.C.; Guo, S.J.; Li, Y.X.; Zhou, H.Y. Microstructure and properties of SiC<sub>p</sub>/Al electronic packaging materials fabricated by pseudo-semi-solid thixoforming. *J. Univ. Sci. Technol. Beijing* **2014**, *36*, 489–495.
17. He, X.X.; Yan, F.Y.; Liu, Z.H.; Li, X. Effects of SiC particles with varied granulrity combination on microstructure and properties of high volume SiC<sub>p</sub>/Al composites. *Spec. Cast. Nonferr. Alloy.* **2015**, *35*, 742–745. (In Chinese)
18. Liu, J.Y.; Liu, Y.C.; Liu, G.Q.; Yin, Y.S.; Shi, Z.L. Oxidation behavior of silicon carbide particales and their interfacial characterization in aluminum matrix composite. *Trans. Nonferr. Met. Soc. China* **2002**, *12*, 961–966.
19. Wang, Y.W. The Microstructures and Properties of SiC<sub>p</sub>/Al Matrix Composites Prepared by Reciprocating Extrusion. Master's Thesis, Xi'an University of Technology, Xi'an, China, 24 March 2009.
20. Lee, J.M.; Lee, S.K.; Hong, S.J.; Kwon, Y.N. Microstructures and thermal properties of A356/SiC<sub>p</sub> composites fabricated by liquid pressing method. *Mater. Des.* **2012**, *37*, 313–316. [[CrossRef](#)]
21. Lee, J.C.; Ahn, J.P.; Shim, J.H.; Shi, Z.; Lee, H.I. Control of the interface in SiC/Al composites. *Scr. Mater.* **1999**, *41*, 895–900. [[CrossRef](#)]
22. Aghajanian, M.K.; Rocazella, M.A.; Burke, J.T.; Keck, S.D. The fabrication of metal matrix composites by a pressureless infiltration technique. *J. Mater. Sci.* **1991**, *26*, 447–454. [[CrossRef](#)]
23. Ren, S.; He, X.; Qu, X.; Humail, I.S.; Li, Y. Effect of Mg and Si in the aluminum on the thermo-mechanical properties of pressureless infiltrated SiC<sub>p</sub>/Al composites. *Compos. Sci. Technol.* **2007**, *67*, 2103–2113. [[CrossRef](#)]
24. Masayuki, M.; Yoshiharu, T.; Akio, K. Thermal Expansion Behavior of SiC<sub>p</sub>/Aluminum alloy composites fabricated by a low-pressure infiltration process. *Mater. Trans.* **2004**, *45*, 1769–1773.
25. Shi, F.; Qing, D.F.; Wu, S.H. The analyses of interracial reactions of SiC<sub>p</sub>/Al System by XRD and Thermodynamic. *Bull. Chin. Ceram. Soc.* **2003**, *6*, 12–16.
26. Viala, J.C.; Bosselet, F.; Laurent, V.; Lepetitcorps, Y. Mechanism and kinetics of the chemical interaction between liquid aluminium and silicon-carbide single crystals. *J. Mater. Sci.* **1992**, *28*, 5301–5312. [[CrossRef](#)]
27. Carotenuto, G.; Arpaia, G.; Nicolais, L. Erosion of reinforcement particles in SiC/aluminum composites. *Appl. Compos. Mater.* **1994**, *1*, 449–463. [[CrossRef](#)]
28. Gui, M.; Kang, S.B.; Euh, K. Thermal conductivity of Al–SiC<sub>p</sub> composites by plasma spraying. *Scr. Mater.* **2005**, *52*, 51–56. [[CrossRef](#)]
29. Hasselman, D.P.H.; Donaldson, K.Y.; Geiger, A.L. Effect of reinforcement particle size on the thermal conductivity of a particulate-silicon carbide-reinforced aluminum matrix composite. *J. Mater. Sci. Lett.* **1992**, *12*, 420–423. [[CrossRef](#)]
30. Tian, R.Z.; Wang, Z.T. *Aluminum and its Working Hand Book*; Central South University: Changsha, China, 2000; pp. 155–169.
31. Lynch, J.F.; Spindel, R.C.; Ching-Sang, C.; Miller, J.H.; Birdsall, T.G. *Effective Thermal Conductivity of Composites with Interfacial Thermal Barrier Resistance*; Springer: New York, NY, USA, 1989; pp. 508–515.
32. Molina, J.M.; Prieto, R.; Narciso, J.; Louis, E. The effect of porosity on the thermal conductivity of Al–12 wt % Si/SiC composites. *Scr. Mater.* **2009**, *60*, 582–585. [[CrossRef](#)]



33. Chu, K.; Jia, C.; Tian, W.; Liang, X.; Chen, H.; Guo, H. Thermal conductivity of spark plasma sintering consolidated SiC<sub>p</sub>/Al composites containing pores: Numerical study and experimental validation. *Compos. Part A Appl. Sci. Manuf.* **2010**, *41*, 161–167. [[CrossRef](#)]
34. Gao, W.; Jia, C.; Jia, X.; Liang, X.; Chu, K.; Zhang, L.; Huang, H.; Liu, M. Effect of processing parameters on the microstructure and thermal conductivity of diamond/Ag composites fabricated by spark plasma sintering. *Rare Met.* **2010**, *29*, 625–629. [[CrossRef](#)]
35. Gencer, A.; Aksu, E.; Nezir, S.; Celebi, S.; Yanmaz, E.; Ates, A.; Shen, Y.L. Combined effects of microvoids and phase contiguity on the thermal expansion of metal-ceramic composites. *Mater. Sci. Eng. A* **1997**, *237*, 102–108.
36. Zhang, Q.; Wu, G.; Jiang, L.; Chen, G. Thermal expansion and dimensional stability of Al-Si matrix composite reinforced with high content SiC. *Mater. Chem. Phys.* **2003**, *82*, 780–785. [[CrossRef](#)]
37. Geiger, A.L.; Jackson, M. Low-expansion MMCs boost avionics. *Adv. Mater. Process.* **1989**, *136*, 23–30.
38. Elomari, S.; Skibo, M.D.; Sundarajan, A.; Richards, H. Thermal expansion behavior of particulate metal-matrix composites. *Compos. Sci. Technol.* **1998**, *58*, 369–376. [[CrossRef](#)]
39. Vaidya, R.U.; Chawla, K.K. Thermal expansion of metal-matrix composites. *Compos. Sci. Technol.* **1994**, *50*, 13–22. [[CrossRef](#)]
40. Luan, B.F.; Pei, Y.F.; Huang, T.L.; Ye, Q.; Huang, G.J.; Yang, Q. Fabrication and thermal expansion properties of particle reinforced Al matrix composites. *J. Chongqing Univ.* **2010**, *33*, 136–142.
41. Zhang, X.; Chen, T.; Qin, H.; Wang, C. A comparative study on permanent mold cast and powder thixoforming 6061 aluminum alloy and SiC<sub>p</sub>/6061Al composite: Microstructures and mechanical properties. *Materials* **2016**, *9*, 407. [[CrossRef](#)]



© 2016 by the authors; licensee MDPI, Basel, Switzerland. This article is an open access article distributed under the terms and conditions of the Creative Commons Attribution (CC-BY) license (<http://creativecommons.org/licenses/by/4.0/>).